Journal of Molecular and Cellular Cardiology Plus 2 (2022) 100023

Contents lists available at ScienceDirect

Journal of Molecular and Cellular Cardiology Plus

journal homepage: https://www.journals.elsevier.com/journal-of-molecular-and-cellular-cardiology-plus

A gradient of force generation at rest differentiates cardiomyopathy outcomes with variants of actin located at the same residue

Michael R. Jones *, Chau Tran [1], Jaskerat Singh [1], John F. Dawson

Department of Molecular & Cellular Biology, University of Guelph, Guelph, ON N1G 2W1, Canada
Centre for Cardiovascular Investigations, University of Guelph, Guelph, ON N1G 2W1, Canada

ARTICLE INFO

Keywords:
Actin
Cardiovascular disease
Mutation
Hypertrophic cardiomyopathy
Dilated cardiomyopathy
Sarcomere
Tropomyosin
Troponin

ABSTRACT

The calcium sensitivity hypothesis helps explain the development of different forms of cardiomyopathy: increased sensitivity to calcium in cardiac sarcomeres leads to hypertrophic cardiomyopathy (HCM) and decreased sensitivity results in dilated cardiomyopathy (DCM). This hypothesis has driven the development of next generation drugs targeting sarcomere proteins to correct the amount of force generated as a result of changes in calcium sensitivity (*e.g.* mavacamten decreases cardiac myosin activity to treat HCM). Characterization of variants of cardiac actin (ACTC) found in patients with HCM or DCM has generally supported the calcium sensitivity hypothesis. Of interest are two different substitution mutations at R312 on ACTC: R312H leads to DCM, while R312C was found in patients with HCM. To determine how changes in the same codon on the same gene lead to different disease phenotypes, we characterized recombinant R312H- and R312C-ACTC variant proteins. Both variants exhibited the same change in calcium sensitivity, suggesting that a factor other than calcium sensitivity is responsible for disease differentiation. We observed a gradient of increased residual myosin activity with R312-ACTC variant proteins under relaxing conditions which may trigger different disease development. Our findings suggest that factors other than calcium sensitivity may contribute to cardiomyopathy development and should be considered when planning treatments.

1. Introduction

Cardiovascular disease (CVD) is currently the leading cause of death globally and imposes significant economic burden [1]. A group of inherited CVD is cardiomyopathies (CM), diseases that result in structural changes of the heart muscle [2]. Cardiomyopathies are categorized into two forms at opposite ends of a spectrum of phenotypes: hypertrophic cardiomyopathy (HCM) with thickening of the left ventricular (LV) septum and dilated cardiomyopathy (DCM) with thinning of the LV wall.

Several hypotheses have been posited to explain the onset of cardiomyopathies. The calcium sensitivity hypothesis states that CMs result from opposite changes in the same activities of heart muscle contraction [3]: HCM results from increases in calcium sensitivity and/or force production, while DCM results from reductions in these activities. A model from Davis et al. produced a tension based model to predict which form of cardiomyopathy will manifest as well as the severity of the disease [4]. In this model, integrated tension curves are placed on a scale above or below 0 (arbitrarily assigned to wildtype). Higher integrals for the tension curves were representative of HCM, while those below 0 were representative of DCM with the magnitude of the value being indicative of a more sever CM onset. There is no unifying hypothesis for CM onset as of now, but the common factor amongst all is that there is a change in actomyosin activity causing these changes.

Nevertheless, these hypotheses are based on the action of the core contractile proteins in muscle sarcomeres: thick filaments of force-generating myosin that bind thin filaments of actin, regulated by tropomyosin and calcium-sensing troponin on the actin filaments. Of the genes encoding these critical proteins, the *ACTC1* gene for cardiac actin was the first to be found with changes associated with cases of either HCM or DCM. This observation sparked the hypothesis that single gene mutations expressing differences in the severity of changes account for the spectrum of observed disease phenotypes [5].

We have suggested that changes in different protein interactions with ACTC might lead to different phenotypes, categorizing actin changes according to the sarcomere proteins they most likely interfere with [6,7]. In general, the biochemical activities of proteins encoded by *ACTC1* mutations agree with the calcium sensitivity hypothesis. This hypothesis suggests that HCM can be treated with next generation drugs that inhibit force production by targeting myosin (such as mavacamten, MYK-461) [8] or reduce calcium sensitivity by targeting troponin (*e.g.* N-(6-aminohexyl)-5-chloro-1-naphthalenesulfonamide, W7) [9], while DCM can be treated with myosin activators or calcium sensitizers (*e.g.* Omecamtiv Mecarbil (OM) and 3-

DOI of original article: http://dx.doi.org/10.1016/j.jmccpl.2022.100025.
* Corresponding author at: Department of Molecular & Cellular Biology, University of Guelph, Guelph, ON N1G 2W1, Canada.
E-mail address: mjones29@uoguelph.ca (M.R. Jones).
[1] These authors were undergraduate researchers.

http://dx.doi.org/10.1016/j.jmccpl.2022.100023
Received 13 June 2022; Received in revised form 21 November 2022; Accepted 27 November 2022

chlordiphenylamine (3-Cl-DPA) respectively) [10,11]. However, there exists mutations that display changes that run counter to the calcium sensitivity hypothesis or have extraneous factors to consider outside of calcium sensitivity such as A331P [12].

There are challenges to this precision medicine approach of targeting the molecular cause of CMs; of concern is the spectrum of phenotypes of CM in general. Even when a mutation causes a shift in contraction, long term effects can complicate diagnosis and treatment; for example, approximately 10–20 % of HCM cases are believed to progress into DCM (known as H-DCM) [13,14]. Thus, a case of DCM might have two different molecular causes, complicating treatment with targeted next generation drugs. Also, as mentioned previously, some ACTC1 variants do not behave with the typical calcium sensitivity hypothesis. Therefore, we need to determine the molecular cause of CMs, studying *ACTC1* to ensure we know the cause for CM onset prior to treatment of the disease with novel therapeutics.

Here, we examine an intriguing pair of *ACTC1* substitution mutations at the same codon (R312) that lead to DCM or HCM (numbering based on the post-translationally processed protein). The R312H ACTC variant found in patients ranging in age from 2 years to 36 years of age was amongst the first linked to DCM [15], while the R312C ACTC variant was discovered in paediatric patients with HCM a decade later [16].

How do two different disease phenotypes result from a single change on one residue on the same protein? The R312 residue stabilizes part of the interface between subdomain 3 and 4 of actin (Fig. 1A) through a network of electrostatic interactions (Fig. 1B) and influences several sites on actin that interact with tropomyosin, aligning with the hypothesis that changes in regulatory protein activity affecting calcium sensitivity are involved. Two hypotheses for disease differentiation are possible: 1) the mutations lead to different phenotypes from onset, or 2) the mutations result in HCM first, with the expression of R312H-ACTC progressing to H-DCM over time. Based on hypothesis #1, R312H ACTC will produce less force and reduced calcium sensitivity, while the R312C variant will result in the opposite effects. With hypothesis #2, both R312-ACTC variants will produce increased force and calcium sensitivity, reflecting an HCM onset disease phenotype. We would then suggest that in a heart expressing R312H-ACTC, the initial HCM phenotype progresses to DCM over time. The finding of both R312H and R312C-encoding *ACTC1* mutations in paediatric patients with DCM or HCM supports option #1, assuming that there is not enough time for DCM to develop from HCM in a 2-year-old patient.

Previous research with recombinant R312H actin variants purified from different systems with varying purification methods suggested reduced stability might contribute to disease. Work with baculovirus-expressed

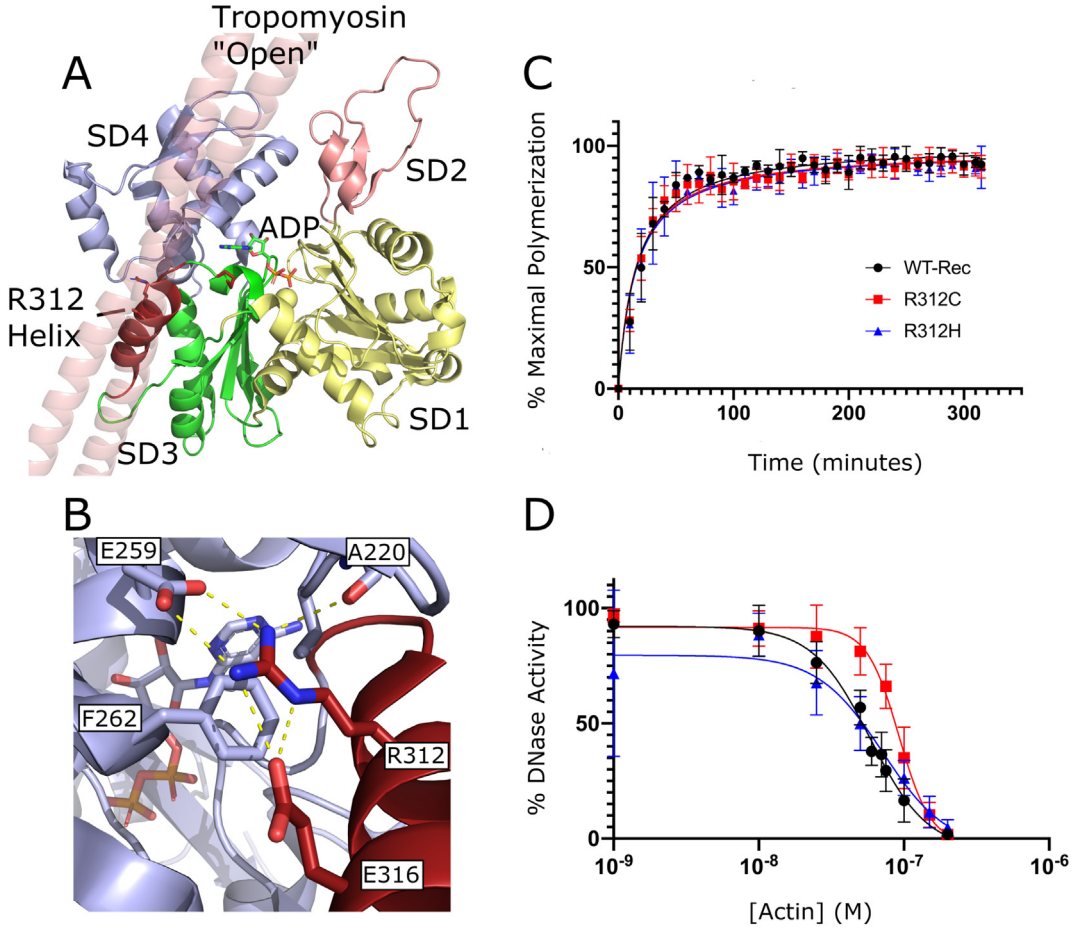

Fig. 1. Actin R312 structural significance and intrinsic properties. A. Depiction of tropomyosin in the open state with the four subdomains of actin coloured in light yellow, light pink, light green and light blue respectively. The helix in which R312 resides is depicted in dark red using PDB 5NOJ [40] The R312 sidechain and ADP nucleotide are shown as a stick models. B. Image of the electrostatic interactions the R312 residue with residues in the vicinity using PDB 5NOJ [40]. Dotted yellow lines depict direct electrostatic interactions, while pi-electron interactions with F262 result from stacking with R312. C. Polymerization curves of 5 μM ACTC proteins containing 15 % pyrene-actin (N = 3 where N is equivalent to the elongation numbers from one cuvette during the reading). Three biological replicates were performed (Biological replicate is equivalent to one purification of the recombinant ACTC). The elongation rates of the R312 mutants were not statistically different to that seen for WT-ACTC (One-Way Anova w/ Post-hoc Tukey Test). Error bars represent SEM. D. Comparison of the DNase-I inhibition by R312 ACTC variants compared to WT-ACTC fit using [inhibitor] *vs* response – Variable slope (four parameters) function on Graphpad Prism. See Table 1 for derived IC_{50} values. (N = 3 where N is equivalent to the average of three technical replicates from one assay). Three biological replicates were utilized (Biological replicate is equivalent to separate purifications of the recombinant ACTC). The IC_{50} of the R312 mutants were not statistically different to that seen for WT-ACTC (One-Way Anova w/ Post-hoc Tukey Test). Error bars represent SEM.

R312H-ACTC resulted in lower maximal myosin sliding velocity, aligning with the calcium sensitivity hypothesis [23]; however, an observed increase in calcium sensitivity in this work runs counter to the hypothesis that R312H-ACTC should possess decreased calcium sensitivity, raising further questions about how DCM results from the R312H-causing mutation. Research has also been published recently on the R312H mutation [17]. No major differences between R312H- and wildtype (WT)-ACTC calcium sensitivity were observed based on observing ATPase stimulation. However, reduced calcium sensitivity was observed with fluorescence-based assays measuring tropomyosin movement across the filament which aligns with our findings in this paper observing calcium sensitivity with *in vitro* motility movement. The hypothesis suggested by Hassoun et al. (2022) is that R312H has a weakened C-state interacting with tropomyosin explaining why they observe changes with the tropomyosin movement across the filament.

To address the question of how HCM or DCM develops from variations of the same amino acid on ACTC, we purified baculovirus-expressed R312H- or R312C-ACTC using gelsolin 4–6 affinity chromatography and examined actin protein function and stability. Using *in vitro* motility (IVM) assays and ATPase assays, we measured myosin interactions with unregulated thin filaments and regulated thin filaments where changes in calcium sensitivity could be observed. Importantly, we observed the same changes in calcium sensitivity for both R312-ACTC variants in accordance with hypothesis #2; however, both R312-ACTC variants exhibited reduced calcium sensitivity suggestive of a DCM phenotype, where hypothesis #2 requires both R312-ACTC variants express a hypersensitive HCM phenotype. Therefore, changes in calcium sensitivity do not explain how R312-ACTC variants lead to different disease phenotypes; some other factor must differentiate these two R312-ACTC variants. Our results suggest that different force output under low load and constitutive myosin activity under relaxing conditions may represent new indicators and mechanisms for DCM and HCM differentiation that could impact precision treatments for patients.

2. Results

2.1. Intrinsic properties

A polymerization assay was performed to assess the impact of the R312H- or R312C-ACTC substitution mutations on the ability of the protein to form filaments (Fig. 1C). We found that the polymerization kinetics did not differ amongst the variants, contrary to previous R312H-ACTC polymerization kinetic studies [6].

Stability of the actin filaments may also play a role in determining disease onset of individuals containing R312-ACTC substitution mutations. The R312-ACTC variants behaved similar to wildtype (WT-ACTC) with R312C-ACTC having a slightly lower melting temperature than WT- and R312H-ACTC (Table 1).

Alterations in the DNase-I binding loop of actin may suggest structural abnormalities resulting from amino acid substitutions in the protein overall. A DNase-I inhibition assay was performed to assess changes in the IC_{50} of R312-ACTC variants and WT-ACTC. We found R312H-ACTC inhibited DNase-I with a similar IC_{50} to WT-ACTC, while R312C-ACTC inhibited DNase-I at a higher IC_{50} value than WT-ACTC (Fig. 1D &Table 1).

Table 1
Intrinsic actin stability. Summary of the stability assays for the ACTC variants R312C and R312H. (N = 3 where N is equivalent to the average of three technical replicates). Three biological replicates were utilized (Biological replicate is equivalent to separate purifications of the recombinant ACTC). The T_m of the R312 variants was not statistically different to that seen for WT-ACTC ($p < 0.05$). The IC_{50} of the variants was not statistically significant ($p < 0.05$) in comparison to WT-ACTC. (One-Way Anova w/ Post-hoc Tukey Test.) Values are plotted as the average ± SEM. These assays are used to assess intrinsic stability changes as well as the IC_{50} of the DNase-I inhibition assessing structural abnormalities.

Intrinsic assays	WT	R312C	R312H
Thermal shift T_m (°C)	59.0 ± 0.58	57.6 ± 0.62	59.4 ± 0.29
Dnase-I inhibition IC_{50} (nM)	60.2 ± 3.97	97.1 ± 8.40	79.3 ± 21.91

2.2. Actomyosin properties

Unregulated actomyosin activity was measured using *in vitro* motility (IVM) and chemical ATPase assays. With increasing ATP concentrations (Fig. 2A), R312H-ACTC presented the highest velocity in IVM assays, followed by R312C- and WT-ACTC. Under saturating ATP concentrations and increasing concentrations of ACTC proteins, we found that R312C- and R312H-ACTC displayed increased ATPase rates relative to WT-ACTC, with R312C-ACTC having the highest ATPase rate of the two variants (Fig. 2B & Table 2).

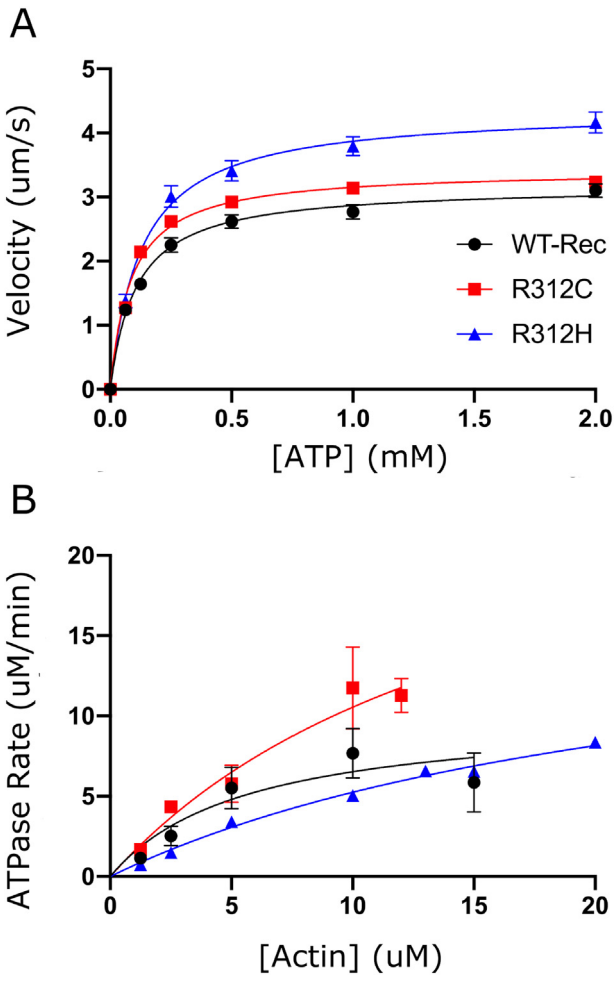

Fig. 2. Unregulated parameters of R312 ACTC variants interacting with myosin. For experiments described in panels A, N = 9, where N is equivalent to the average of ten filaments from one video at each ATP concentration. For panel B, N = 3, where N is the average of three technical replicates from an enzymatic plate assay. Three separate preparations of protein were used for each assay. Error bars represent SEM. A. Michaelis-Menten curves of gliding velocities of the ACTC protein at increasing concentrations of ATP in the IVM assay. The K_M of the R312 variants were not statistically different to that seen for WT-ACTC but were statistically different between each other. The V_{max} of R312H was statistically significant ($p < 0.05$) in comparison to WT-ACTC and R312C (One-Way Anova w/ Post-hoc Tukey Test, see Table 2). B. Michaelis-Menten curves of myosin ATPase rate in the presence of increasing concentrations of ACTC protein and 2 mM ATP. Data was fit against the Michaelis-Menten function in Graphpad Prism. The K_M and V_{max} of the R312 variants were not statistically different to that seen for WT-ACTC (One-Way Anova w/ Post-hoc Tukey Test, see Table 2).

Unregulated frictional load assays were performed with R312-ACTC variant proteins to assess activity when acting against an alpha-actinin load force (Fig. 3). Non-linear curve fitting performed as previously described [18] revealed that R312H-ACTC had the significantly lower displacement force while R312C-ACTC displacement force was significantly higher (Table 2). Briefly, the model extrapolating the driving force of the myosin bed utilized in the IVM assay is made from a set of parameters/assumptions that are unique to the IVM assay such as actin filament length, attachment, detachment rates, *etc*.

2.3. Regulated filament properties

IVM and ATPase assays were performed with ACTC filaments regulated by troponin and tropomyosin under saturating ATP and varying calcium concentrations. With ATPase assays, R312C- and R312H-ACTC both displayed similar decreases in pCa_{50} values reflected in rightward shifts in their pCa curves (Fig. 4A). Similar rightward shifts were also observed in IVM assays, with similar maximal activities when compared to WT-ACTC (Fig. 4B & Table 3). Interestingly, we observed more motile filaments and higher average filament velocities under relaxing conditions (pCa 10) for R312H- and R312C-ACTC than WT-ACTC protein (Fig. 4C), with R312H-ACTC filaments displaying significantly higher qualities in both parameters.

3. Discussion

3.1. Intrinsic properties

Previous research with the R312H-ACTC variant revealed protein structural instability, with yeast expressing R312H *act1* growing abnormally, *in vitro* translation of R312H-actin resulting in a defective folding pattern, and recombinant R312H-ACTC protein displaying altered polymerization kinetics, DNase-I binding and melting temperatures [6,19,20]. Our results here, however, do not reflect major changes in overall actin structure for either the R312C- or R312H-ACTC proteins compared to WT-ACTC, with similar polymerization rates, melting temperatures and DNase-I inhibition IC_{50} values.

The differences we see compared to previous studies may be due to the current G4-6 purification technique which does not rely on partial denaturation of actin in formamide to release it from DNase-I binding followed by refolding in the presence of high ATP concentrations. While our current findings do not support major structural changes with R312-ACTC, it is important to note that R312H-ACTC protein did exhibit changes previously when compared to other ACTC variants following DNase-I purification, supporting the hypothesis that the R312 position is important for refolding of actin suggested in previous *in vitro* translation experiments [20]. However, changes in protein stability do not differentiate the R312-ACTC variants from each other enough to explain different disease states.

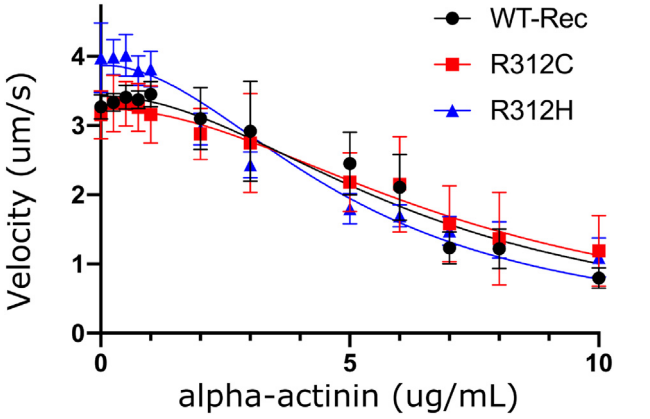

Fig. 3. Unregulated frictional load IVM assay using alpha-actinin. For experiment described below, N = 9 where N is equivalent to the average of ten filaments from one video at each alpha-actinin concentration. Three separate protein preparations were used for the experiments and error bars shown represent SEM. Gliding velocities of the ACTC variants at increasing concentrations of alpha-actinin (μg/mL) were determined and data fit against a previously described equation [18]. The F_d of the R312 mutants were not statistically different to that seen for WT-ACTC but were statistically different between each other (One-Way Anova w/ Post-hoc Tukey Test, see Table 2).

3.2. Actomyosin properties

Since R312H-ACTC is found in DCM patients and R312C-ACTC in HCM patients, we went on to characterize the interaction of myosin with the R312-ACTC variants with the hypothesis that opposite actomyosin activities would explain opposite disease progression. However, our results showed that R312C- and R312H-ACTC generally exhibited actomyosin interactions similar to those of WT-ACTC with no obvious opposite changes between the variants, although we did observe a V_{max} of R312H-ACTC about 37 % higher than that of WT-ACTC (Table 2).

To assess if this increase in velocity with R312H-ACTC was maintained under load we performed unregulated frictional load assays. With increasing concentrations of alpha-actinin adding more load, we saw higher IVM sliding velocities with R312H-ACTC under low load, which decreased at a greater rate with increasing load to similar velocities seen with R312C- and WT-ACTC. This change in velocity under load suggests that the force output of actomyosin with R312H-ACTC when acting against a load force is not as high as actomyosin with R312C-ACTC.

The F_d derived from modeling the data showed a discrepancy between the R312-ACTC variants compared to WT, with R312H-ACTC displaying a lower F_d and the R312C-ACTC trending higher. F_d represents the driving force of the myosin molecules in the interactions that is opposed by the frictional force of alpha-actinin binding and is often considered a measure of isometric force. While tempting to suggest that changes in velocity under load may represent a distinguishing factor for cardiomyopathy onset, it is important to note that unregulated actomyosin systems do not always tell the full story. Prior research has shown that actomyosin activity of unregulated systems can deviate from regulated systems including troponin and tropomyosin [21,22]. Therefore, we performed regulated assays containing troponin and tropomyosin to gain a portrait of the full scope of potential changes with R312-ACTC variants in heart muscle.

Table 2
Unregulated assay results. Summary of the unregulated assays for the ACTC variants R312C and R312H. (N = 9 for IVM assays where N is equivalent to the average of ten filaments in a video.) Three ACTC purifications were utilized three times for data collection. (N = 3 for the ATPase assays where N is the average of 3 technical replicates) The V_{max} in the IVM assay of the R312H variant is statistically different to that seen for WT-ACTC (*$p < 0.05$). In addition, the V_{max} of the R312 variants in the assay were statistically significant between one another ($^{\S}p < 0.05$). The R312 variants were not significantly different from WT-ACTC for their K_M values but were significantly different from each other ($^{\S}p < 0.05$). No statistical significance was seen for the ATPase variables. The F_d from the Frictional load IVM also found statistical significance between the R312 variants ($^{\S}p < 0.05$) but not to WT-ACTC. (One-Way Anova w/ Post-hoc Tukey Test.) Values are listed as the average ± SEM.

Unregulated assay	WT	R312C	R312H
IVM			
V_{max} (μm/s)	3.18 ± 0.11	3.43 ± 0.077§	4.37 ± 0.16*,§
K_M (mM)	0.108 ± 0.0034	0.089 ± 0.010§	0.130 ± 0.0046†,§
ATPase			
V_{max} (μM/s)	10.2 ± 3.18	28 ± 11.9	18.25 ± 3.06
K_M (μM)	5.633 ± 4.05	16.56 ± 10.97	24.8 ± 6.15
Frictional IVM			
F_d (pN)	249.4 ± 22.7	335.9 ± 73.9§	174.0 ± 11.9§

† $p < 0.10$.

3.3. Regulated filament properties

We performed regulated actomyosin assays to investigate the differences between R312H- and R312C-ACTC variants and found that both ACTC variants had similar changes in pCa curves relative to WT-ACTC, disproving the hypothesis that opposite changes should be observed if ACTC changes trigger different disease phenotypes from onset.

R312H-ACTC has been studied previously with full-length myosin [23] where an increase in calcium sensitivity coupled with reduced maximal IVM sliding velocities was observed. This increase in calcium sensitivity runs counter to our work here where the pCa curves of both regulated R312-ACTC variants in IVM and ATPase assays indicated decreased calcium sensitivity. These results also run counter to the calcium sensitivity hypothesis. There is literature prior to this which also contradicts the calcium sensitivity hypothesis where HCM and DCM display similar calcium sensitivity characteristics [24–26]. Interestingly, our current R312H-ACTC results are confirmed by another recent study examining this variant using similar methods [27], suggesting differences in methods may account for the disparity in results. The main differences are in the ACTC protein purification process (cycles of polymerization *vs* G4-6 affinity chromatography) and the use of full-length myosin where we and Erdmann use HMM in IVM assays.

Further work with purified R312H-ACTC protein was performed by Hassoun et al. [17]. Their pCa curves were plotted from enzyme-coupled myosin S1-ATPase assays and showed no differences under relaxing conditions, where we saw increased activity in our single molecule studies. Single molecule studies allow us to measure the activity of individual actin filaments, whereas differences in molecular activity from a subpopulation are averaged out in bulk enzymatic assays. Changes in filament length and fragility may cause differences in filament gliding velocity; however, differences in filament length were not noted in our motility experiments, nor did we measure differences in the polymerization curves of these ACTC variants suggestive of breakage or reduced polymerization (Fig. 1).

In addition to the calcium sensitivity hypothesis, there is evidence that protein-protein interactions and post-translational modifications play a big role in actomyosin activity. Reductions in the phosphorylation of cardiac Troponin-I (cTnI) and myosin-binding protein C (cMyBP-C) have shown increases in calcium sensitivity [28,29]. Taken together, there is clear evidence that there is more to the cardiomyopathy onset with the R312 variants than just calcium sensitivity and the interactions with these external factors may help to explain the changes we see here.

Aside from those differences, one characteristic of our IVM assays caught our attention. Under relaxing conditions at pCa10, we do not expect to see any significant motility in IVM assays as all filaments should be inhibited from interacting with myosin. However, we noted that both R312-ACTC variants displayed more motility under relaxing conditions compared to WT-ACTC (Fig. 4C) with R312H-ACTC displaying more than R312C-ACTC. The velocities of those filaments followed a similar pattern to the maximal velocities of unregulated filaments (Fig. 2A) with R312H-ACTC being higher than WT-ACTC while R312-ACTC filaments displayed velocities like WT-ACTC. We suggest a hypothesis where a gradient in the strength of contraction under relaxing conditions distinguishes between HCM and DCM brought on with R312-ACTC variants: low relaxing

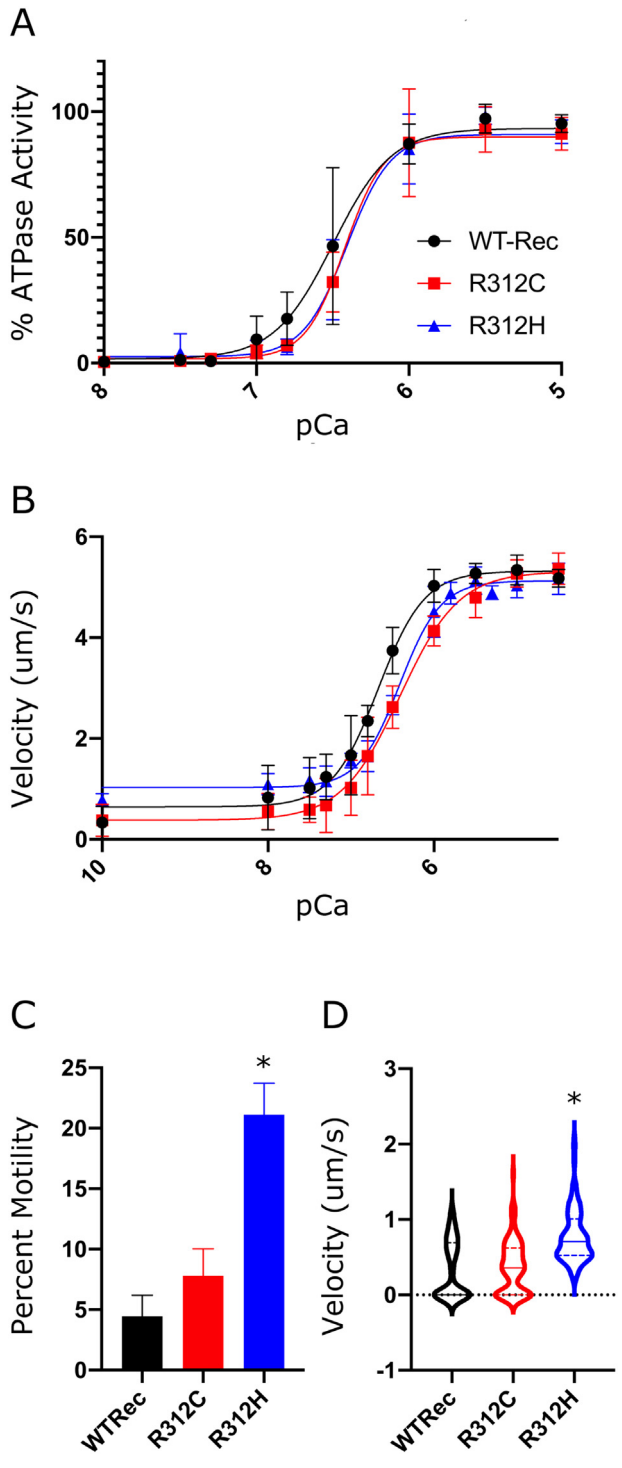

Fig. 4. Regulated R312-ACTC variant interactions with myosin. For experiment described in panel A, N = 3, where N is equivalent to the average of three technical replicates from a single enzymatic plate assay. In panel B, N = 9, where N is the average of ten filaments from a single video at each pCa level. Three separate protein purifications were used for the experiments and error bars represent SEM. A. pCa curves as a function maximal myosin ATPase activity. The pCa_{50} of the R312 mutants were not statistically different to that seen for WT-ACTC, neither were the Hill-Coefficients (One-Way Anova w/ Post-hoc Tukey Test, see Table 3). B. pCa curves as a function of the gliding velocity of filaments moving in *in vitro* motility assays. The pCa_{50} of the R312 mutants was statistically different to that seen for WT-ACTC while the V_{max} of the variants was not statistically significant ($p < 0.05$) in comparison to WT-ACTC. Hill coefficients were statistically different between the variants, but not in comparison to WT-ACTC (One-Way Anova w/ Post-hoc Tukey Test, see Table 3). C. Bar graph of percent motile filaments per video (N = 9), motile were taken as velocities > 0.25 μm/s at pCa 10 for regulated IVM assays. Bars represent the mean percent motility with error bars representing SEM. The mean percent motile R312H filaments were significantly different than WT-ACTC and R312C-ACTC. *$p < 0.05$ determined by One-Way Anova w/ Post-hoc Tukey Test. D. Violin plot of gliding velocity of all filaments at pCa 10 for regulated IVM assays (N = 90). Solid line represents the median while the dashed lines represent the quartiles. As opposed to WT-ACTC and R312C-ACTC where some filaments showed no movement, all R312H-ACTC filaments exhibited a velocity greater than zero. The velocities of R312H filaments were significantly different than WT-ACTC and R312C-ACTC. *$p < 0.05$ determined by One-Way Anova w/ Post-hoc Tukey Test.

Table 3
Regulated assay results. Summary of the regulated assays for the ACTC variants R312C and R312H. (N = 9 for IVM assays where N is equivalent to the average of ten filaments in a video.) Three ACTC purifications were utilized three times for data collection. (N = 3 for the ATPase assays where N is the average of 3 technical replicates.) The V_{max} in the IVM assay of the R312 variants was not statistically different to that seen for WT-ACTC. The Hill Coefficient of the R312 variants in the IVM assay were statistically significant between one another ($^{\S}p < 0.05$) while there was slight significance for the R312H variant compared to WT-ACTC ($^{\dagger}p < 0.10$). The R312 variants were significantly different from WT-ACTC for their pCa_{50}values ($*p < 0.05$) but were not significantly different from each other. No statistical significance was seen for the ATPase variables. (One-Way Anova w/ Post-hoc Tukey Test.) Values are listed as the average ± SEM.

Regulated assay	WT	R312C	R312H
IVM			
V_{max} (μm/s)	5.34 ± 0.063	5.34 ± 0.094	5.15 ± 0.053
Hill Coefficient	1.50 ± 0.11	1.32 ± 0.15§	1.90 ± 0.12†,§
pCa_{50}	6.70 ± 0.036	6.41 ± 0.042*	6.41 ± 0.020*
ATPase			
Hill Coefficient	3.52 ± 0.79	4.06 ± 1.19	3.45 ± 0.53
pCa_{50}	6.48 ± 0.13	6.4 ± 0.067	6.38 ± 0.082

contraction with R312C-ACTC results in concentric hypertrophy of cardiomyofibres and HCM, while high relaxing contraction with R312H-ACTC leads to eccentric growth and DCM.

Our results bring to light two factors that contribute to different disease progression with R312-ACTC variants: changes in calcium sensitivity and constitutive myosin activity under relaxing conditions. Both factors are the result of altered regulatory protein interactions with actin; response to calcium on one hand and modulating myosin binding in the absence of calcium on the other. In the absence of calcium, tropomyosin blocks myosin binding to actin filaments; however, with the R312-ACTC variants, low-level activity under relaxing conditions suggests that tropomyosin binding has been altered. It may also suggest a change in the binding state of tropomyosin for the R312 variants. For example, if the variants destabilize the Tropomyosin B-state (blocked) conformation, we may see heightened activity under low calcium. This altered B-state conformation has been seen previously with Troponin mutations [30]. Future work could examine the binding affinity of tropomyosin for the R312-ACTC variants, while unitary force measurements with laser trapping could shed light on differences in force output. In addition, *in silico* analysis of the binding landscape of Tropomyosin may shed light on if the energetics of Tropomyosin interactions have been altered as done previously with M305L-ACTC [31].

Current therapeutics targeting myosin or troponin specifically can correct changes in force because of calcium sensitivity alteration; however, our discovery of a range of constitutive myosin activity under relaxing conditions contributing to HCM or DCM development complicates the prescription of current therapeutics. A myosin activator could correct the lower force typically observed with DCM; however, prescribing a myosin activator for DCM resulting from elevated resting actomyosin activity would amplify the pathological change. Our work here shows the importance of understanding the molecular causes of disease to develop and administer precision therapeutics.

3.4. Limitations

While this study contains insight into the biochemical properties of the R312C- and R312H-ACTC variants, there are other factors which can also be assessed to obtain a complete picture of the underlying cause of cardiomyopathy onset. Future experiments could include: *in silico* structural and energy analyses, *in vivo* studies with transgenic animals harboring cardiac actin mutations, and reconstituted myofibre force transduction experiments, similar to what was done previously with M305L-ACTC [31].

One model for cardiovascular disease that we have experience with is zebrafish [32,33]. Inserting the R312C and R312H mutations into the zebrafish genome allows us to assess cardiac activity, such as heart rate and ejection velocity, to obtain a more rounded picture of how the cardiovascular system as a whole is impacted. Analyses *in silico* would allow us to assess structural changes by exploring flexibility changes over the whole molecule. Localized changes in flexibility, as shown by Viswanathan et al. 2020 can inform a hypothesis regarding the impact of protein-protein interactions changes. [31].

In our work, we focussed on the biochemical properties of the R312-ACTC variant proteins, allowing us to test one hypothesis for disease onset. With this approach, we can address the issues of calcium sensitivity and force output individually, free of other complicating factors which would exist at the whole organism level.

4. Experimental procedures

4.1. Reagents

All reagents, unless otherwise specified, were purchased from Fisher Scientific (Whitby, ON).

4.2. Protein purification

All recombinant ACTC proteins were produced using a baculovirus expression system. The recombinant ACTC proteins were expressed in *Sf*9 insect cells infected with recombinant baculoviruses containing the *ACTC1* variant of interest and purified with hexa-His-tagged gelsolin segments 4-6 (G4-6) as described previously [21]. Tropomyosin and troponin was purified from bovine cardiac ether powder as outlined previously [34,35]. The myosin utilized for the *in vitro* motility and ATPase assays was purified from rabbit muscle which was then cleaved into heavy mero-myosin (HMM) using α-chymotrypsin as previously outlined [36]. Bovine cardiac actin used in purification of HMM was purified from left ventricular tissue as described [37].

4.3. Protein stability assays

4.3.1. Thermal shift assay

Purified ACTC proteins were first dialyzed into G-buffer (2 mM Tris (pH 8), 0.2 mM $CaCl_2$, 0.2 mM ATP, 0.5 mM–beta-mercaptoethanol, 0.002 % NaN_3) overnight, changing the buffer three times. This ACTC protein was then diluted in Thermal-buffer (1x-SYPRO orange, topped with G-buffer) to 0.4 mg/mL. 20 μL of this solution was added in triplicate to a 96 RT-PCR well plate and sealed with an optical adhesive cover. These samples were then analysed using a thermal cycler, with the lowest of the negative derivative readings being the melting temperature. This analysis was performed for all recombinant ACTC samples using three biological replicates.

4.3.2. Actin polymerization assays

Purified ACTC proteins in G-buffer were diluted to 5 μM in 90 μL total G-buffer. 85 % of this concentration was the ACTC variant of interest and 15 % was actin previously labelled with pyrene as described [38]. The proteins were added to a quartz cuvette and placed in a Cary Eclipse Fluorescence Spectrophotometer with settings of 347 nm excitation, 407 nm emission, 5 nm slit width. Once roughly 5 min of initial readings were measured to establish a baseline, 10 μL of 10× poly buffer (250 mM Tris (pH 8), 500 mM KCl, 10 mM EGTA, 20 mM $MgCl_2$, 1 mM ATP) were added to each cuvette. The readings were continued for 400 min total to obtain the plateau of the polymerization curve. The readings were saved in an excel spreadsheet and plotted.

4.3.3. DNase-I inhibition assay

Purified ACTC proteins in G-buffer were diluted to their respective concentrations in G-buffer lacking sodium azide. DNase-I from Worthington was further purified by Superdex-200 gel filtration in buffer A (2 mM Tris, pH 8.0, 0.2 mM $CaCl_2$, 50 mM NaCl, 0.5 mM beta-mercaptoethanol). DNase-I is incubated at 140 nM with increasing concentrations of ACTC (1–200 nM) at room temperature for 30 min. Add 100 μL of DNase-I incubation to 100 μL of 24 μg/μL salmon sperm DNA and assess absorbance at

260 nm at 2 s intervals for 3 min. Activity is normalized from 0 to 100 % and plotted.

4.4. In vitro motility assays

For assays measuring the velocity and movement of F-actin composed of different ACTC variants, ACTC proteins in G-buffer were polymerized with 10× poly-buffer to an effective concentration of 1× poly-buffer.

Active HMM was isolated by "deadheading" where HMM was bound to bovine cardiac F-actin in the absence of nucleotide. Active HMM was then released by the addition of 2 mM ATP and collected in the supernatant fraction following centrifugation at 95,000 rpm for 15 min in a TLA110 rotor (Beckman, Palo Alto, CA). This bind-and-release process was repeated three times, resulting in purified and active HMM in the final supernatant.

The flow cells utilized for actin visualization were produced by adding nitrocellulose-covered coverslips and double-sided tape to a microscope slide. The deadheaded HMM was diluted to 0.25 mg/mL in 1× AB (20 mM imidazole (pH 8.0), 10 mM KCl, 2 mM $MgCl_2$, 1 mM DTT, 2 mM ATP (pH 8.0), and 1 mM EGTA (pH 8.0)) and bound to the coverslip of the flow cell. Remaining binding sites on the coverslip were then blocked with 0.1 mg/mL BSA in 1× AB buffer. The flow cell was then washed with 1× AB.

For unregulated F-actin assays, 1000× diluted rhodamine-phalloidin-labelled ACTC protein was added to the flow cells and washed with 1×AB. The activating buffer (20 mM imidazole (pH 8), 10 mM KCl, 2 mM $MgCl_2$, 1 mM DTT, 1 mM EGTA) was added with concentrations of ATP increasing from 0 mM to 2 mM. Filament movement was analysed using Image J as described previously [22] and velocities at each ATP concentration were plotted with GraphPad Prism 6, and fitted by non-linear regression to determine the K_M and V_{max} of the corresponding Michaelis-Menten curve.

For regulated thin filament assays, a similar experimental set up was used; however, 3 μM troponin and tropomyosin were added to the flow cell following ACTC addition, washing after their addition with 1× AB. The pCa buffers of 10–4.5 (desired pCa, 20 mM imidazole (pH 8), 10 mM KCl, 2 mM $MgCl_2$, 1 mM DTT, 1 mM EGTA, and 2 mM ATP) were added. Both the filament velocity and percentage of filaments moving at each pCa was quantified and plotted against the pCa value in GraphPad Prism 6. The corresponding pCa curve was fitted by utilizing a log(agonist) *vs* response - Variable slope (four parameters) curve fit to provide the pCa_{50} for the ACTC variant studied.

4.5. Data/statistical analysis

4.5.1. Protein stability and ATPase assays

Recombinant ACTC was purified separately 3 times with each purification being used as a single biological replicate. Within each 96 well plate assay, the individual concentrations were performed in triplicate as 3 technical replicates which are averaged to a single N value. This was performed with 3 different protein purifications (N = 3). Each point was inputted into GraphPad Prism 8 by Dotmatics (San Diego, CA). Each assay was analysed with a different regression model. The unregulated assays were analysed using the Michaelis Menten Non-linear regression model. The regulated assays were analysed using the log(agonist) *vs* response – variable slope (four parameters) non-linear regression model. The DNase-I inhibition assay were analysed with [inhibitor] *vs* response – variable slope (four parameters) non-linear regression model. The regression models output the results listed in the corresponding tables (±SEM). Statistical analysis was performed on the output results to assess if the differences in the variants were statistically significant from wildtype-ACTC or from each other. The regression results output from the analysis were analysed in triplicate for each biological replicate (N = 3) using a one-way ANOVA. A subsequent Tukey post-hoc test was done between all means if any differences were found. Corresponding p-values were listed in the corresponding tables if significance was found between the groups.

4.5.2. IVM assays

Data collection was done similarly to previous literature using IVM assays [39]. Briefly, three purifications were completed for the IVM assays. Three videos for each condition were captured for each preparation (N = 9). The velocity of 10 filaments from each video were averaged and inputted into GraphPad Prism 8 by Dotmatics (San Diego, CA) as a single replicate. The unregulated assays were analysed using the Michaelis Menten Non-linear regression model. The regulated assays were analysed using the log(agonist) *vs* response – variable slope (four parameters) non-linear regression model. The frictional load assays was analysed using a previously-described equation (REF). The resulting regression model outputs are listed in Tables 2 and 3 (±SEM). Statistical analyses were performed on the output results to assess if the differences between the variants were statistically significant from wildtype-ACTC or from each other. The regression coefficients output from the analyses were analysed for each replicate (N = 9) using a one-way ANOVA. A subsequent Tukey post-hoc test was performed between all means if differences were found. Corresponding p-values are listed in the corresponding tables if significance was found between the groups.

CRediT authorship contribution statement

MRJ and JFD designed the experiments. CT performed and analysed unregulated myosin ATPase experiments, JS performed and analysed DNase-I inhibition assay, MRJ performed and analysed all other experiments. MRJ and JFD wrote the manuscript.

Declaration of competing interest

The authors declare the following financial interests/personal relationships which may be considered as potential competing interests: John Dawson reports financial support was provided by Heart and Stroke Foundation of Canada.

Acknowledgements

This work was funded by a Heart and Stroke Foundation of Canada Grant-in-Aid to JFD (G-18-0020424).

References

[1] Heidenreich PA, Trogdon JG, Khavjou OA, Butler J, Dracup K, Ezekowitz MD, et al. Forecasting the future of cardiovascular disease in the United States: a policy statement from the American Heart Association. Circulation. 2011;123:933–44.
[2] Braunwald E. Cardiomyopathies: an overview. Circ Res. 2017;121:711–21.
[3] Teng GZ, Dawson JF. The dark side of actin: cardiac actin variants highlight the role of allostery in disease development. Arch Biochem Biophys. 2020;695:108624.
[4] Davis J, Davis LC, Correll RN, Makarewich CA, Schwanekamp JA, Moussavi-Harami F, et al. A tension based model distinguishes hypertrophic versus dilated cardiomyopathy. Cell. 2016;165:1159.
[5] Seidman JG, Seidman C. The genetic basis for cardiomyopathy: from mutation identification to mechanistic paradigms. Cell. 2001;104:557–67.
[6] Mundia MM, Demers RW, Chow ML, Perieteanu AA, Dawson JF. Subdomain location of mutations in cardiac actin correlate with type of functional change. PLoS One. 2012;7:1–8.
[7] Despond EA, Dawson JF. Classifying cardiac actin mutations associated with hypertrophic cardiomyopathy. Front Physiol. 2018;9:405.
[8] Olivotto I, Oreziak A, Barriales-Villa R, Abraham TP, Masri A, Garcia-Pavia P, et al. Mavacamten for treatment of symptomatic obstructive hypertrophic cardiomyopathy (Explorer-HCM): a randomised, double-blind, placebo-controlled, phase 3 trial. Lancet. 2020;396:759–69.
[9] Oleszczuk M, Robertson IM, Li MX, Sykes BD. Solution structure of the regulatory domain of human cardiac troponin C in complex with the switch region of cardiac troponin I and W7: the basis of W7 as an inhibitor of cardiac muscle contraction. J Mol Cell Cardiol. 2010;48:925–33.
[10] Teerlink JR, Diaz R, Felker GM, McMurray JJV, Metra M, Solomon SD, et al. Cardiac myosin activation with omecamtiv mecarbil in systolic heart failure. N Engl J Med. 2021;384:105–16.
[11] Tikunova SB, Cuesta A, Price M, Li MX, Belevych N, Biesiadecki BJ, P.J. 3-Chlorodiphenylamine activates cardiac troponin by a mechanism distinct from bepridil or TFP. J Gen Physiol. 2019;151:17.

[12] Bai F, Caster HM, Rubenstein PA, Dawson JF, Kawai M. Using baculovirus/insect cell expressed recombinant actin to study the molecular pathogenesis of HCM caused by actin mutation A331P. J Mol Cell Cardiol. 2014;74:64–75.
[13] Elliott P, McKenna WJ. Hypertrophic cardiomyopathy. Lancet. 2004;363:1881–91.
[14] Ommen S, Nishimura R. Hypertrophic cardiomyopathy. Curr Probl Cardiol. 2004;29:239–91.
[15] Olson TM, Michels VV, Thibodeau SN, Tai YS, Keating MT. Actin mutations in dilated cardiomyopathy, a heritable form of heart failure. Science. 1998;280:750–2.
[16] Kaski JP, Syrris P, Esteban MTT, Jenkins S, Pantazis A, Deanfield JE, et al. Prevalence of sarcomere protein gene mutations in preadolescent children with hypertrophic cardiomyopathy. Circ Cardiovasc Genet. 2009;2:436–41.
[17] Hassoun R, Erdmann C, Schmitt S, Fujita-Becker S, Mügge A, Schröder RR, et al. Functional characterization of cardiac actin mutants causing hypertrophic (p. A295S) and dilated cardiomyopathy (p.R312H and p.E361G). Int J Mol Sci. 2022;23:4465.
[18] Greenberg MJ, Moore JR. The molecular basis of frictional loads in the in vitro motility assay with applications to the study of the loaded mechanochemistry of molecular motors. 2010;67:285.
[19] Wong WW, Doyle TC, Cheung P, Olson TM, Reisler E. Functional studies of yeast actin mutants corresponding to human cardiomyopathy mutations. J Muscle Res Cell Motil. 2001;22:665–74.
[20] Vang S, Corydon TJ, Børglum AD, Scott MD, Frydman J, Mogensen J, et al. Actin mutations in hypertrophic and dilated cardiomyopathy cause inefficient protein folding and perturbed filament formation. FEBS J. 2005;272:2037–49.
[21] Liu H, Henein M, Anillo M, Dawson JF. Cardiac actin changes in the actomyosin interface have different effects on myosin duty ratio. Biochem Cell Biol. 2017;96:1–24.
[22] Teng GZ, Shaikh Z, Liu H, Dawson JF. M-class hypertrophic cardiomyopathy cardiac actin mutations increase calcium sensitivity of regulated thin filaments. Biochem Biophys Res Commun. 2019;519:148–52.
[23] Debold EP, Saber W, Cheema Y, Bookwalter CS, Trybus KM, Warshaw DM, VanBuren P. Human actin mutations associated with hypertrophic and dilated cardiomyopathies demonstrate distinct thin filament regulatory properties in vitro. J Mol Cell Cardiol. 2010;48:286–92.
[24] Sequeira V, Wijnker PJM, Nijenkamp LLAM, Kuster DWD, Najafi A, Witjas-Paalberends ER, et al. Perturbed length-dependent activation in human hypertrophic cardiomyopathy with missense sarcomeric gene mutations. Circ Res. 2013;112:1491–505.
[25] Sequeira V, Najafi A, Wijnker PJM, Dos Remedios CG, Michels M, Kuster DWD, Van Der Velden J. ADP-stimulated contraction: a predictor of thin-filament activation in cardiac disease. Proc Natl Acad Sci U S A. 2015;112:E7003–12.
[26] Nakano SJ, Walker JS, Walker LA, Li X, Du Y, Miyamoto SD, Sucharov CC, et al. Increased myocyte calcium sensitivity in end-stage pediatric dilated cardiomyopathy. Am J Physiol Heart Circ Physiol. 2019;317:H1221–30.
[27] Hassoun R, Schmitt S, Kikuti C, Houdusse A, Mazur AJ, Erdmann C. Integration of cardiac actin mutants causing hypertrophic (p.A295S) and dilated cardiomyopathy (p.R312H and p.E361G) into cellular structures. Antioxidants. 2021;10:1082.
[28] Konhilas J, Irving TC, Wolska BM, Jweied EE, Martin AF, Solaro J, de Tombe PP. Troponin I in the murine myocardium: influence on length-dependent activation and interfilament spacing. J Physiol. 2003;547:951–61.
[29] Stelzer JE, Patel JR, Moss RL. Protein kinase A-mediated acceleration of the stretch activation response in murine skinned myocardium is eliminated by ablation of cMyBP-C. Circ Res. 2006;99:884–90.
[30] Kobayashi T, Solaro RJ. Increased Ca2+ affinity of cardiac thin filaments reconstituted with cardiomyopathy-related mutant cardiac troponin I. J Biol Chem. 2006;281:13471–7.
[31] Viswanathan MC, Schmidt W, Franz P, Rynkiewicz MJ, Newhard CS, Madan A, et al. A role for actin flexibility in thin filament-mediated contractile regulation and myopathy. Nat Commun. 2020;11:1–15.
[32] González-Rosa JM. Zebrafish models of cardiac disease: from fortuitous mutants to precision medicine. Circ Res. 2022;130:1803–26.
[33] Ojehomon M, Alderman SL, Sandhu L, Sutcliffe S, Van Raay T, Gillis TE, Dawson JF. Identification of the actc1c cardiac actin gene in zebrafish. Prog Biophys Mol Biol. 2018;138(138):32–7.
[34] Greaser ML, Gergely J. Reconstitution of troponin activity from three protein components. J Biol Chem. 1971;246:4226–33.
[35] Tobacman LS, Adelstein RS. Mechanism of regulation of cardiac actin-myosin subfragment 1 by troponin-tropomyosin. Biochemistry. 1986;25:798–802.
[36] Margossian SS, Lowey S. Preparation of myosin and its subfragments from rabbit skeletal muscle. Methods Enzymol. 1982;85:55–71.
[37] Spudich JA, Watt S. The regulation of rabbit skeletal muscle contraction: I. Biochemical studies of the interaction of the tropomyosin-troponin complex with actin and the proteolytic fragments of myosin. J Biol Chem. 1971;246:4866–71.
[38] Zigmond SH. In vitro actin polymerization using polymorphonuclear leukocyte extracts. Methods Enzymol. 2000;325:237–54.
[39] Schmidt W, Madan A, Brian Foster D, Cammarato A. Lysine acetylation of F-actin decreases tropomyosin-based inhibition of actomyosin activity. J Biol Chem. 2020;295:15539.
[40] Risi C, Eisner J, Belknap B, Heeley DH, White HD, Schröder GF, Galkin VE. Ca2+-induced movement of tropomyosin on native cardiac thin filaments revealed by cryoelectron microscopy. Proc Natl Acad Sci U S A. 2017;114:6782–7.